ACS chemical biology

Articles

pubs.acs.org/acschemicalbiology

Murgocil is a Highly Bioactive Staphylococcal-Specific Inhibitor of the Peptidoglycan Glycosyltransferase Enzyme MurG

Paul A. Mann,[†] Anna Müller,[‡] Li Xiao,[§] Pedro M. Pereira,[∥] Christine Yang,[⊥] Sang Ho Lee,[†] Hao Wang,[†] Joanna Trzeciak,[†] Jonathan Schneeweis,[#] Margarida Moreira dos Santos,[∥] Nicholas Murgolo,[▽] Xinwei She,[○] Charles Gill,[◆] Carl J. Balibar,[†] Marc Labroli,[⊥] Jing Su,[⊥] Amy Flattery,[◆] Brad Sherborne,[§] Richard Maier,[¶,☆] Christopher M. Tan,[†] Todd Black,[†] Kamil Önder,[¶,☆] Stacia Kargman,[#] Frederick J Monsma, Jr.,[#] Mariana G. Pinho,[∥] Tanja Schneider,[‡,■] and Terry Roemer*[,†]

[†]Infectious Disease Research, Merck Research Laboratories, Kenilworth, New Jersey 07033, United States

[‡]Institute of Medical Microbiology, Immunology and Parasitology—Pharmaceutical Microbiology Section, University of Bonn, Bonn, Germany

[§]Computational Chemistry, Global Structure Chemistry, Merck Research Laboratories, Kenilworth, New Jersey 07033, United States

[∥]Laboratory of Bacterial Cell Biology, Instituto de Tecnologia Química e Biológica, Universidade Nova de Lisboa, Avenida da República, 2781-901 Oeiras, Portugal

[⊥]Medicinal Chemistry, Merck Research Laboratories, Kenilworth, New Jersey 07033, United States

[#]*In Vitro* Pharmacology, Merck Research Laboratories, Kenilworth, New Jersey 07033, United States

[▽]Research Solutions, Bioinformatics, Merck Research Laboratories, Kenilworth, New Jersey 07033, United States

[○]Informatics IT, Merck Inc., Boston, Massachusetts 02110, United States

[◆]*In Vivo* Pharmacology, Merck Research Laboratories, Kenilworth, New Jersey 07033, United States

[¶]Procomcure Biotech GmbH, Krems a.d. Donau, Austria

[☆]Division of Molecular Dermatology, Department of Dermatology, Paracelsus Medical University, Salzburg, Austria

[■]German Centre for Infection Research (DZIF), partner site Bonn-Cologne, Bonn, Germany

Supporting Information

ABSTRACT: Modern medicine is founded on the discovery of penicillin and subsequent small molecules that inhibit bacterial peptidoglycan (PG) and cell wall synthesis. However, the discovery of new chemically and mechanistically distinct classes of PG inhibitors has become exceedingly rare, prompting speculation that intracellular enzymes involved in PG precursor synthesis are not 'druggable' targets. Here, we describe a β-lactam potentiation screen to identify small molecules that augment the activity of β-lactams against methicillin-resistant *Staphylococcus aureus* (MRSA) and mechanistically characterize a compound resulting from this screen, which we have named murgocil. We provide extensive genetic, biochemical, and structural modeling data demonstrating both *in vitro* and in whole cells that murgocil specifically inhibits the intracellular membrane-associated glycosyltransferase, MurG, which synthesizes the lipid II PG substrate that penicillin binding proteins (PBPs) polymerize and cross-link into the cell wall. Further, we demonstrate that the chemical synergy and cidality achieved between murgocil and the β-lactam imipenem is mediated through MurG dependent localization of PBP2 to the division septum. Collectively, these data validate our approach to rationally identify new target-specific bioactive β-lactam potentiation agents and demonstrate that murgocil now serves as a highly selective and potent chemical probe to assist our understanding of PG biosynthesis and cell wall biogenesis across Staphylococcal species.

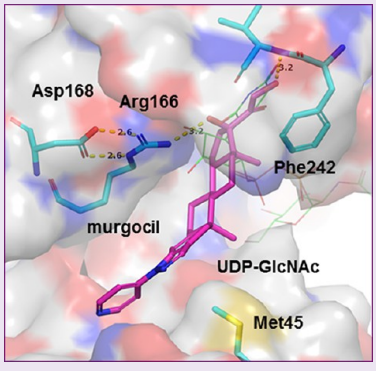

Peptidoglycan (PG) is an essential carbohydrate polymer of the bacterial cell wall, providing strength to resist osmotic pressure, maintaining cell shape, and coordinating cell division and septation. PG is composed of chains of a repeating disaccharide unit comprising *N*-acetyl-glucosamine (GlcNAc) and *N*-acetyl-muramic acid (MurNAc) that are cross-linked by short peptides.[1] The PG monomer is synthesized within the cytoplasm in a multistep process, starting with the conversion of UDP-GlcNAc to UDP-MurNAc through the activities of MurA and MurB. Subsequently, UDP-MurNAc is modified by a

Received: July 2, 2013
Accepted: August 19, 2013
Published: August 19, 2013

 © 2013 American Chemical Society

series of Mur ligases (MurC-F), which sequentially synthesize a pentapeptide comprising L-Ala-D-Glu-L-Lys (or DAP)-D-Ala-D-Ala. This soluble PG precursor is then linked to a lipid carrier (undecaprenyl-phosphate; C_{55}−P) by the membrane protein MraY (resulting in undecaprenyl-P-P-MurNAc-pentapeptide and referred to as lipid I). Completion of PG monomer synthesis is catalyzed by MurG, a membrane-associated nucleotide-sugar glycosyltransferase, which utilizes UDP-GlcNAc substrate to form undecaprenyl−P-P-GlcNAc-MurNAc-pentapeptide, or lipid II.[1,2] Following species-specific modifications and export to the cell surface, lipid II serves as the substrate for a family of penicillin binding proteins (PBPs) that, depending on their specific activity, polymerize linear chains of the PG polymer via transglycosylation (TG) of disaccharide units and/or cross-link adjacent PG polymers by transpeptidation (TP) of their peptide side chains.[1−3] β-lactam antibiotics such as penicillins, cephalosporins, and carbapenems act as irreversible competitive inhibitors of PBP enzymes, thereby blocking PG synthesis and cross-linking leading to cell lysis.[4]

Staphylococcus aureus, a leading cause of serious Gram-positive bacterial infections, has become alarmingly resistant to β-lactams and now reflects over 50% of clinical isolates reported in the U.S.A. and throughout the world.[5,6] *S. aureus* has four PBPs (PBP1−4), each susceptible to β-lactam inhibition.[3] Methicillin-resistant *S. aureus* (MRSA) strains are broadly resistant to β-lactams due to the acquisition of the *mecA* gene, encoding an additional PBP (PBP2A) with intrinsically low binding affinity to β-lactams.[7−11] MRSA evades the action of β-lactams by the cooperative function of PBP2 providing TG activity and PBP2A providing the necessary TP/cross-linking activity to maintain PG synthesis.[3,9,12,13] However, in addition to PBP2 and PBP2A, a large number of accessory factors are required for the full expression of β-lactam resistance of MRSA and many of these are, in fact, PG synthesis enzymes responsible for lipid II synthesis and modification.[14−18] Cognate inhibitors to such targets are particularly attractive from the perspective of developing combination agents, which if paired with β-lactams are synergistic and restore the activity of β-lactams against MRSA.[17−22]

Surprisingly, no other clinically successful agents targeting non-PBP enzymes involved in PG biosynthesis have been developed, although fosfomycin, which targets MurA activity, has limited clinical utility.[23] In fact, even the discovery of small molecules displaying whole cell bioactivity and which clearly target specific enzymes involved in intracellular steps of PG monomer biosynthesis has been exceedingly rare and is limited to liposidomycin targeting MraY[24−26] and D-cycloserine, which inhibits alanine racemase and D-Ala-D-Ala ligase enzymes that catalyze the synthesis of MurF substrate.[23] Noteworthy, all PG inhibitors described are derived from natural products and conspicuously absent are reports of synthetic compounds with potent whole cell activity and rigorous mechanism-of-action (MOA) evidence describing target-specific inhibition of any enzyme involved in PG lipid II synthesis. Indeed, the paucity of bioactive target-specific inhibitors to the PG pathway has left many to question whether enzymes involved in lipid II synthesis are druggable.[23,27]

Here, we describe a phenotypic screen for synthetic small molecules that potentiate the activity of β-lactam antibiotics against MRSA. We identify the steroid-like compound we have named murgocil and demonstrate it to be a highly selective inhibitor of MurG, abolishing the conversion of lipid I to lipid II *in vitro* and impairing PG synthesis in drug treated cells. Further, murgocil resistance mutations isolated in MRSA and *Staphylococcus epidermidis* map exclusively to *murG*, revealing the MOA of murgocil in a whole cell context across β-lactam susceptible and resistant *Staphylococci* spp. and demonstrating that these mutations are sufficient to confer MurG-based murgocil resistance *in vitro*. Docking studies using a homology model of *S. aureus* MurG based on the *Escherichia coli* MurG crystal structure[28,29] and Staphylococcal murgocil MurG amino acid substitution mutations predict that murgocil binds to a deep cleft within the MurG protein, resulting in a competition with UDP-GlcNAc substrate as well as potentially locking the enzyme into a rigid, inactive form. Finally, we demonstrate that murgocil is synergistic and cidal in combination with β-lactam antibiotics against MRSA and that mechanistically this is mediated in part by murgocil-dependent delocalization of PBP2 from the division septum and where PG and cell wall biosynthesis normally occurs.

RESULTS AND DISCUSSION

Phenotypic Screen for β-Lactam Synergy Identifies Murgocil. Genetic studies have identified a growing number of auxiliary factors required for MRSA β-lactam resistance since gene deletion or depletion in their expression levels restores MRSA susceptibility to diverse β-lactams.[14−18,30,31] With few exceptions, these factors participate in the coordinated process of cell division and cell wall synthesis, the latter of which involves the synthesis of PG as well as other cell surface polymers, including wall teichoic acid[32,33] and lipoteichoic acid.[34] We and others have demonstrated that small molecule inhibitors of several of these factors are synergistic with β-lactams against MRSA strains.[17−22,30−35] Based on these findings, we initiated a phenotypic screen to empirically identify small molecule inhibitors with synergistic activity in combination with imipenem (IPM), with the expectation that such chemotypes would reflect inhibitors to auxiliary factors involved in MRSA β-lactam resistance.

Previously, we have reported a 20 000 compound library of synthetic small molecules[19] demonstrated to display growth inhibitory activity against MRSA when tested at 8 μM in combination with ertapenem (EPM) at a subminimal inhibitory concentration (4 μg/mL; note this is referred to as the EPM drug resistance breakpoint concentration to which the drug is defined as clinically ineffective against MRSA). EPM was selected instead of IPM at this stage due to its superior stability in liquid medium. However, as this primary assay was performed at a single drug screening concentration in liquid medium, it was not possible to discern whether compounds in the library are bioactive or nonbioactive alone or conclude whether such compounds comprising this bioactive library exhibit additivity or synergy in combination with EPM. To address this issue, we performed a secondary phenotypic screen where MRSA strain COL was seeded into LB agar plates containing either the subminimal inhibitory breakpoint concentration (4 μg/mL) of IPM versus 32 μg/mL MIC of IPM against COL), or mock treatment (2% DMSO) and each plate pair robotically spotted using 1 mM stock solutions of focused library compounds (250 nL compound/spot; 384 compounds/plate) onto the surface of the agar plate. IPM was selected over EPM for performing this secondary screen as it fulfills the preferred potency and spectrum of a desired β-lactam in our combination agent strategy. After 18−24 h incubation, visually comparing the zone of growth inhibition attributed to

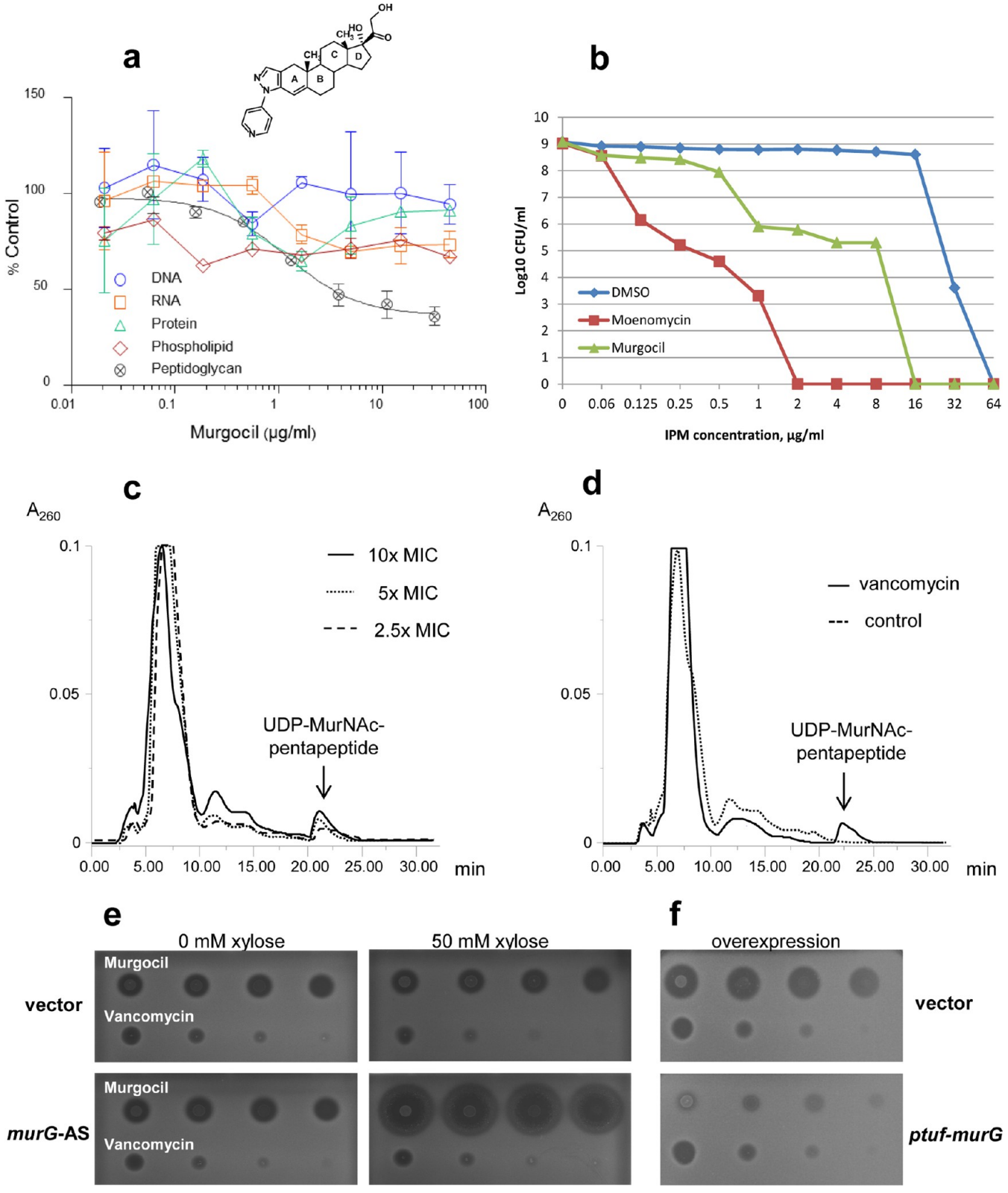

Figure 1. Murgocil inhibits PG biosynthesis. (a) Macromolecular labeling of *S. aureus* strain RN4220 cells treated with murgocil specifically produces a dose dependent depletion of PG synthesis. Chemical structure of murgocil is shown. (b) PAP analysis of MRSA COL treated cells with $^{1}/_{4}$ MIC of murgocil, moenomycin, or mock control (DMSO at 2% final concentration) in combination with a range (0−64 μg/mL) of imipenem (IPM). Chemical synergy is scored by enumerating colony forming units (CFU) post drug treatment. (c, d) *S. aureus* murgocil-treated cells (2.5×, 5×, and 10× MIC; 5, 10, 20 μg/mL) display a dose dependent accumulation of the PG intermediate, UDP-N-acetyl-muramoyl-pentapeptide (UPD-MurNAc-pentapetide) comparable to vancomycin-treated cells at 10 × MIC (5 μg/mL). (e) Antisense-mediated depletion of *murG* expression by 50 mM xylose supplementation (bottom panel) induces MRSA COL hypersensitivity to murgocil versus vector control (top panel) treated cells. (f) MRSA COL maintaining overexpression plasmid ptuf-MurG (bottom panel) displays murgocil dose dependent resistance versus control (top panel) treated cells.

dx.doi.org/10.1021/cb400487f | *ACS Chem. Biol.* 2013, 8, 2442−2451

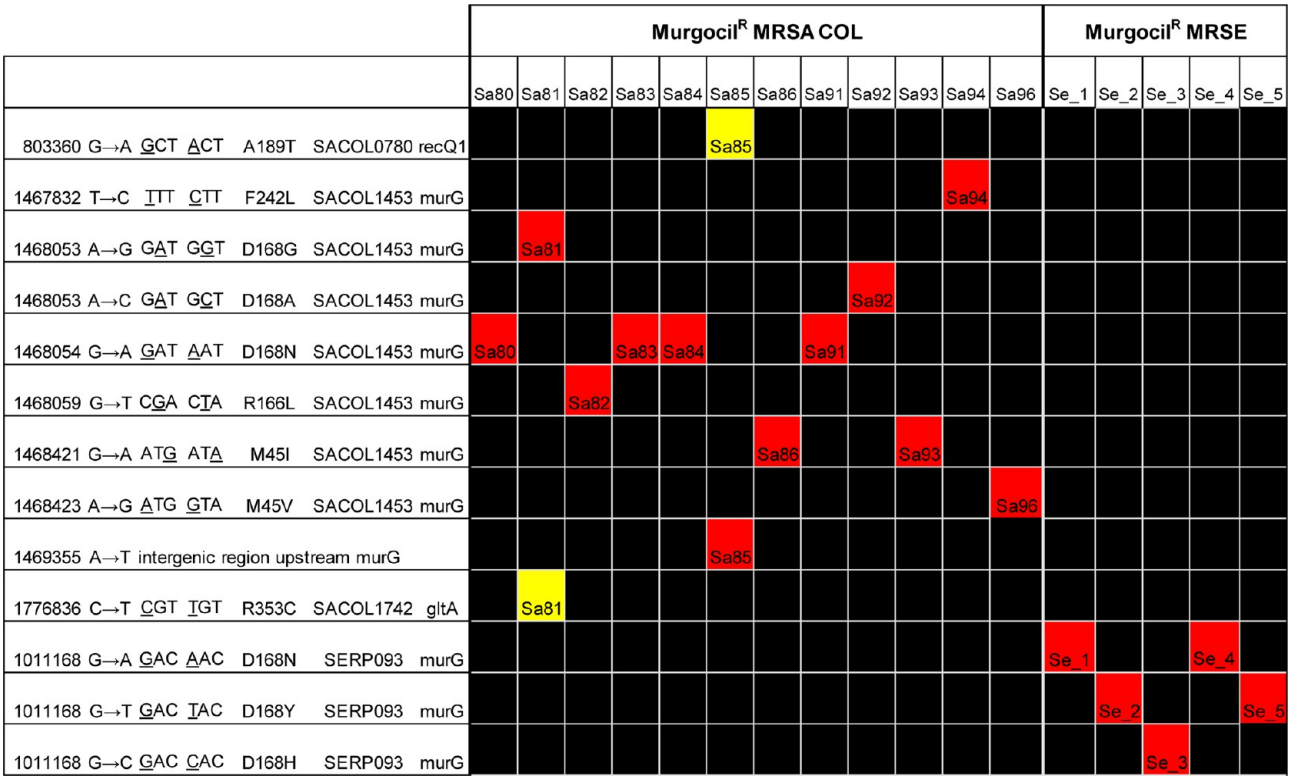

Figure 2. *murG* missense mutations confer murgocil resistance. Heatmap summary of all nonsynonymous mutations identified by illumina-based whole genome sequencing (>100× genome coverage) of 17 independently isolated murgocil drug resistant mutants in MRSA COL and MRSE strain CLB26329. Red, nonsynonymous mutation which maps to *murG*; yellow, additional nonsynonymous mutation identified by whole genome sequencing; black, no change versus parental genome sequence. Genome position, base change, and resulting amino acid substitution are shown. Murgocil mutants Sa80−96 and Se1−5 refer to *S. aureus* and *S. epidermidis* isolates, respectively. Note: additional substitutions (yellow) are presumably unlinked to drug resistance as each strain also contains a MurG amino acid substitution.

each spotted compound between ± IPM supplement provided a simple assessment of each possible chemotype (Supporting Information (SI) Figure 1).

Murgocil Inhibits PG Biosynthesis. Based on their minimum inhibitory concentration (MIC) against MRSA COL in the absence or presence of IPM (4 μg/mL), physicochemical properties, and compound availability, 134 compounds were evaluated further for possible PG inhibitory effects by performing macromolecular labeling (MML) of drug-treated cells. MML was performed in *S. aureus* strain RN4220 by measuring the relative incorporation of radiolabeled precursors of PG versus DNA, RNA, protein, or phospholipid across a range of concentrations. Two potent PG inhibitory compounds were identified. L-108 is a structural analog of CDFI (SI Figure 2 panel f), a previously described PG synthesis inhibitor targeting the *S. aureus* cell wall assembly protein, SAV1754 [19] (and which serves as a positive control for the screen) and murgocil, a steroid-like synthetic compound (Figure 1 panel a). Interestingly, murgocil inhibition was highly selective for PG synthesis; all other macromolecular pathways assayed were unaffected at concentrations up to 20-fold the MIC of murgocil. Further, the murgocil EC50 value (1.5 μg/mL) for inhibiting PG synthesis approaches very closely its MIC against RN4220 (MIC = 2−4 μg/mL; SI Table 1). Corroborating this inhibitory effect on PG synthesis, high pressure liquid chromatography (HPLC) analysis of murgocil-treated *S. aureus* revealed a dose-dependent accumulation of UDP-MurNAc-pentapeptide paralleling the inhibitory effect of vancomycin-treated cells (Figure 1 panel c and d and SI Table 2). Importantly, murgocil also displayed synergistic activity in combination with IPM against MRSA COL both by the standard checkerboard assay (Supplementary Figure 3) as well as by the more sensitive population analysis profiling (PAP) assay, with synergy approaching that of the PBP trans-glycosylation inhibitor, moenomycin [12] (Figure 1 panel b). Further, murgocil displayed a modest cidal (1.5 log kill) effect alone at 8× MIC in a standard *S. aureus* kill curve assay and in combination with IPM at 4 μg/mL, cidality approached that of the bactericidal agent, levofloxacin, with ∼3 log kill achieved within 24 h (SI Figure 3 panel b).

To specifically link murgocil to its cognate target within the PG pathway, 14 MRSA COL strains (see SI Figure 4), each maintaining a unique xylose-inducible antisense (AS) interference plasmid targeting a specific gene involved in PG biosynthesis,[17] were assayed for murgocil hypersensitivity under conditions in which the target is partially depleted. Accordingly, any gene-specific AS-mediated depletion strain displaying marked hypersensitivity to murgocil is a candidate for the target of the compound. One AS strain corresponding to a *murG* knock down uniquely demonstrated a dramatic murgocil hypersensitivity (Figure 1 panel e and SI Figure 4) not observed against a broad assortment of antibiotics and bioactive molecules previously tested.[17,36] To corroborate MurG as the target of murgocil, we also observed that MRSA COL maintaining an autonomously replicating *murG* plasmid, robustly overexpressing MurG (SI Figure 5) was noticeably resistant to the inhibitor (Figure 1 panel f), resulting in an 8-fold higher MIC versus wild type and control strains (SI Figure

dx.doi.org/10.1021/cb400487f | ACS Chem. Biol. 2013, 8, 2442−2451

5). Conversely, MurG overexpression provided no noticeable resistance to all control antibiotics tested (SI Figure 5). These gene dosage effects and highly specific susceptibility changes to murgocil strongly implicate a direct mechanistic relationship between MurG and murgocil.

MurG Amino Acid Substitutions Confer Staphylococcal Target-Based Murgocil Resistance. Drug resistance mutations provide a genome-wide survey of small molecule MOA in a whole cell context and mapping of such mutations by Next Generation Sequencing (NGS) methods has proven highly successful in discerning between target-based and bypass or compensatory drug resistance mutations.[20,37] Therefore, to independently test whether murgocil is the cognate inhibitor of MurG, we isolated 12 stable murgocil resistant mutants in MRSA COL, each demonstrating a MIC increase to >64 μg/mL (versus MIC = 4 μg/mL against wild type MRSA COL) and performed NGS analysis. In all cases, a single missense mutation in *murG* was identified in murgocil resistant isolates, and in all but two instances, no additional nonsynonymous mutations were found elsewhere in their genome (Figure 2). *S. aureus* MurG amino acid substitution mutations map to three regions of the protein: SaMurG-M45I, SaMurG-M45V, SaMurG-R166L, SaMurG-D168A, SaMurG-D168G, SaMurG-D168N, and SaMurG-F242L. No substantial growth defect or altered antibiotic susceptibility phenotype was observed for any of the mutants. Consistent with their robust enzymatic activity when tested *in vitro*, none of the examined MurG mutants exhibited an attenuated virulence phenotype in a murine infection model (SI Figure 6).

We also isolated 5 independent murgocil resistant mutants in the methicillin-resistant *Staphylococcus epidermidis* (MRSE) strain CLB26329 (Figure 2), which represents a second clinically relevant *Staphylococcus* species. MRSE murgocil mutants similarly exhibited substantial (16−32-fold) increases in MIC to murgocil as observed in *S. aureus*. Following whole genome sequencing of these isolates, nonsynonymous mutations again uniquely mapped to *murG* (note *S. aureus* and *S. epidermidis* MurG are >98% identical; see SI Figure 7), with MRSE murgocil resistant mutants being either identical to those identified in MRSA COL (e.g., SeMurG-D168N) or new amino acid substitutions at position 168 (e.g., SeMurG-D168Y or SeMurG-D168H). These data strongly implicate MurG as the direct cellular drug target of murgocil and that *murG* point mutations are causal for target-based murgocil resistance across *Staphylococci* spp.

Murgocil Inhibits MurG Enzymatic Activity. The cytosolic membrane-associated glycotransferase MurG synthesizes lipid II by catalyzing the transfer of N-acetyl glucosamine (GlcNAc) from UDP-N-acetyl glucosamine (UDP-GlcNAc) to the C4 hydroxyl of undecaprenyl-pyrophosphate-N-acetylmuramoyl-pentapeptide (lipid I). Reconstitution of the SaMurG-catalyzed reaction *in vitro*, using purified recombinant enzyme and substrates, lipid I, and (^{14}C)-UDP-GlcNAc, respectively, revealed a full conversion to the synthesis product lipid II, which migrates slower on the TLC compared to lipid I [38] (Figure 3 panel a). Testing murgocil in this system showed that lipid II synthesis is strongly impaired in a dose-dependent fashion (20−400 μM; Figure 3 panel a). An almost complete inhibition of MurG activity was observed in the presence of 3000 μM murgocil and an IC50 of approximately 115 μM was determined under the conditions tested (Figure 3 panel b; see Summary and Implications).

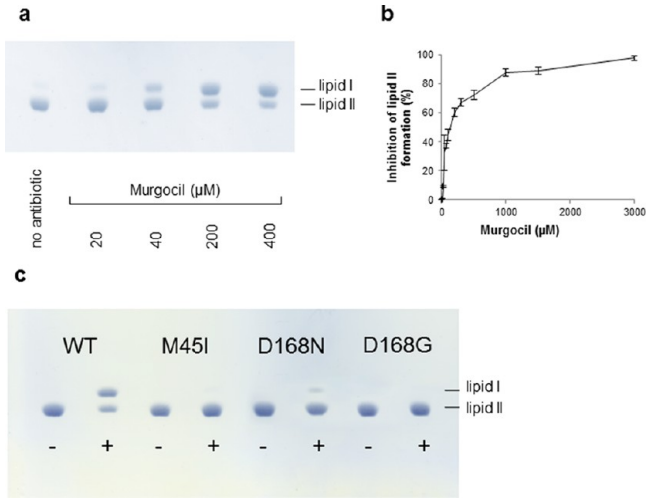

Figure 3. Murgocil inhibits *S. aureus* -catalyzed lipid II synthesis *in vitro*. (a) Murgocil dose dependent inhibition of purified MurG-His$_6$ enzyme activity. Lipid intermediates were extracted from the reaction mixture, separated by TLC and visualized by PMA staining. Murgocil inhibitory effect was tested at concentrations ranging from 0 to 400 μM. (b) Graphical summary of murgocil dose dependent inhibition of MurG-His$_6$ mediated lipid II formation. (c) *S. aureus* MurG-His$_6$ enzymes containing M45I, D168N, and D168G murgocil resistance mutations are active but refractory to murgocil-mediated inhibition of lipid II synthesis. Reactions were performed, as indicated in panel a, at 200 μM murgocil.

To investigate the impact of MurG amino acid substitutions on enzymatic activity and resistance to murgocil, site directed mutagenesis was used to generate recombinant proteins MurG_M45I, MurG_D168N, and MurG_D168G. In line with the *in vivo* situation, amino acid substitutions did not affect MurG enzymatic activity and full conversion to lipid II was achieved *in vitro* (Figure 3 panel c). In contrast to wild type SaMurG, the Lipid II synthesizing activity of all individual MurG variants was unaffected in the presence of 200 μM murgocil (Figure 3 panel c), further confirming that these single amino acid substitutions are causal for murgocil resistant phenotypes and that they prevent a murgocil/MurG interaction without affecting binding of the substrate UDP-GlcNAc.

Structural Modeling of *S. aureus* MurG and Murgocil Binding. As no crystal structure of the *S. aureus* MurG protein is reported, we used a homology model built with the crystal structure of the MurG/UDP-GlcNAc complex of *E. coli*[28,29] as the template to investigate how murgocil likely inhibits MurG as well as the basis of murgocil resistance. SaMurG and EcMurG share 24% sequence identity, and the alignment reveals that most major structure elements as well as the substrate binding site are conserved (SI Figure 7). Indeed, homology modeling predicts SaMurG and EcMurG are highly structurally related, consisting of N- and C-terminal globular domains divided by a large cleft where UDP-GlcNAc substrate occupies part of the space (Figure 4 panel a). Interestingly, the four murgocil mutation sites, M45, R166, D168, and F242 are each located at or near the uracil binding pocket and lined along the cleft between the two domains. Therefore, we modeled murgocil into this cleft and predict it binds deep within this cleft, stacking against the N-terminal and C-terminal domains (Figure 4 panel b). Two hydrogen bonds were observed between murgocil and SaMurG: the D-ring primary hydroxyl group with the backbone NH of V243 and the D-ring

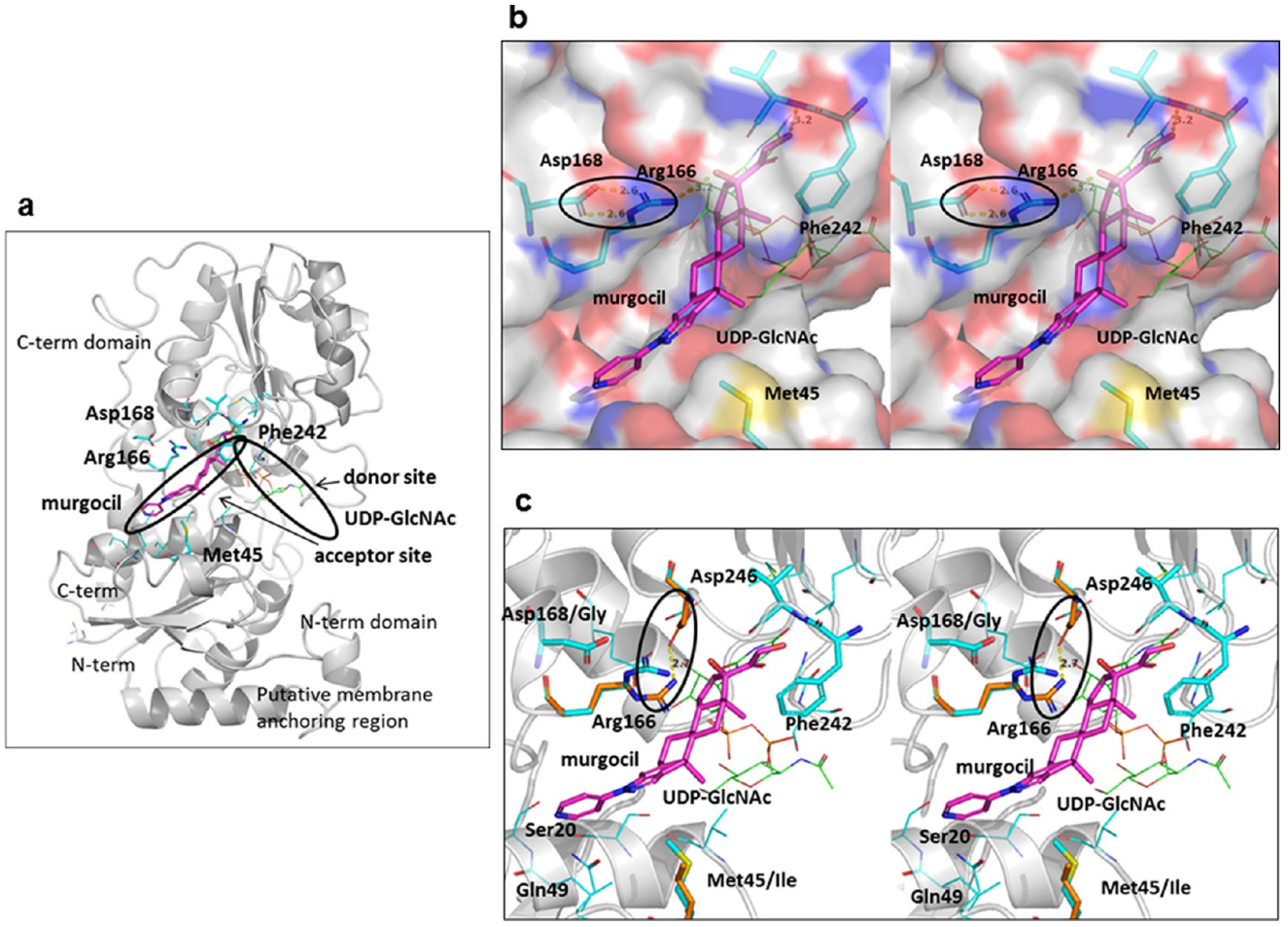

Figure 4. Homology model of SaMurG/murgocil complex and murgocil binding site. (a) murgocil in magenta and UDP-GlcNAc in green were overlaid in the V-shaped cleft of SaMurG marked by gray elipses. Murgocil binding site residues are in cyan. (b) Murgocil binding site with four resistant mutation sites labeled in cyan. Two hydrogen bonds between the murgocil and SaMurG and the salt-bridge of D168 and R166 were displayed with their atomic distances. (c) Murgocil mutations sites and pyridine binding residues were colored in cyan sticks. An altered conformation of the R166 side-chain caused by mutation of D168G or D168N and the new salt-bridge with D246 were delineated in brown, along with M45I mutation. Both panels b and c are in stereo view.

tertiary hydroxyl group with R166 side-chain NH. In this structural model, the F242 (which aligns with F244 in EcMurG) phenyl ring stacks against murgocil, capping the binding pocket of the murgocil D-ring. M45 side-chain is in direct contact with ligand through hydrophobic interactions. Although D168 is not within the predicted ligand binding site, it forms a salt bridge with R166 side-chain and likely indirectly contributes to murgocil binding.

Interestingly, the binding model of murgocil displays an overlap of its D-ring and D-ring substitutions with uracil of the substrate, whereas the rest of the ligand (A-, B-, and C-ring and C-ring substitution) occupies a completely different site from where UDP-GlcNAc binds. Therefore, murgocil and UDP-GlcNAc are predicted to bind largely nonoverlapping regions within a large V shaped cleft, with the uracil site as the vertex of the V and where murgocil and UDP-GlcNAc binding would compete (Figure 4 panel a). However, as this model predicts murgocil also binds extensively within the cleft but distal the uridine binding site, it could also potentially act as an allosteric inhibitor, locking SaMurG into an inactive conformation.

The binding model of murgocil also offers a molecular basis for murgocil resistance resulting from MurG amino acid substitution mutations. First, the M45I mutation is expected to lose favorable hydrophobic interactions with murgocil since the isoleucine side-chain would then be too short to interact with murgocil. Similarly, the R166L mutation would remove hydrogen bond of arginine side-chain NH_2 group with the ligand and the F242L mutation would alter hydrophobic interactions as well as removal of the $\pi-\pi$ stacking between F242 phenyl ring and ligand D-ring substitution groups. Although D168 is predicted not to directly contact murgocil, the salt bridge between D168 and R166 is likely disrupted by the D168G or D168N mutation resulting in the movement of R166 side-chain toward D246 to form a new salt bridge (Figure 4 panel c). This altered side-chain of R166 points into the predicted murgocil binding pocket and would cause VDW conflict with the inhibitor.

PBP2 is Delocalized in Murgocil-Treated Cells. Previously, it has been demonstrated that lipid II is required for proper localization of PBP2 to the division septum where active PG synthesis occurs in *S. aureus*.[3,39] Therefore, the simplest explanation for the extreme hypersensitivity of the *murG* antisense strain to β-lactams and the observed synergy between murgocil and β-lactams is that murgocil-specific inhibition of MurG leads to a depletion of lipid II and consequently PBP2 is delocalized from the septum. To test this,

dx.doi.org/10.1021/cb400487f | *ACS Chem. Biol.* 2013, 8, 2442−2451

we performed localization studies of murgocil-treated cells maintaining a previously described functional superfolder green fluorescent protein (sGFP)-PBP2 fusion gene integrated into the *pbp2* locus of MRSA COL.[20] sGFP-PBP2 correctly localized to the division septum in mock-treated cells as previously reported.[20] However, sGFP-PBP2 was highly delocalized among cells treated with murgocil at 5× MIC for 1 h, with discrete patches of sGFP-PBP2 localized throughout the plasma membrane (Figure 5 panel a) and verified by quantification of fluorescence signal at the septum versus fluorescence at the lateral wall under the two conditions tested (Figure 5 panel a and b). To determine if PBP2 delocalization was a specific effect of the presence of murgocil and consequent decrease of its substrate, and not part of general disassembly of the cell division machinery[40] that could be caused by the presence of the antibiotic, we determined the localization of the FtsZ ring,[20,41] a bacterial ortholog of tubulin, using as a reporter the FtsZ-associated protein EzrA.[42] MRSA COL cells expressing a functional copy of EzrA-mCherry showed septal rings both in the absence and in the presence of murgocil (Figure 5 panel a and b), indicating that murgocil-dependent delocalization of PBP2 is not due to disassembly of the divisome.

Fluorescence localization studies of MRSA COL expressing a functional copy of MurG-GFP integrated into the *murG* locus were also unaffected by murgocil treatment, with the fusion protein localized at the plasma membrane, as indicated by patches of strong fluorescence, similar to untreated cells (Figure 5 panel a). Therefore, murgocil appears unlikely to interfere with the normal membrane-association of MurG, an observation consistent with the fact that murgocil resistance mutations do not map to the proposed membrane-association interface of MurG.[28] We conclude that murgocil-based delocalization of PBP2 involves depletion of lipid II rather than disruption of the Z ring. In addition, we propose that the synergy between murgocil and β-lactams involves (at least in part) murgocil-mediated depletion of lipid II substrate, which is required for both PG synthesis and proper localization of PBP2, and that the concomitant mislocalization of PBP2 under these conditions renders cells susceptible to reduced β-lactam concentrations that are now sufficient to inactivate the residual functionally competent PBP2 activity remaining at the septum.

Summary and Implications. Here, we describe a MRSA whole cell β-lactam potentiation screen resulting in the identification of the highly specific PG inhibitor, murgocil, targeting the broadly conserved and essential glycosyltransferase, MurG. Murgocil is demonstrated to inhibit PG synthesis based on MML profiling as well as HPLC analysis revealing the accumulation of UDP-MurNAc-pentapeptide in drug-treated cells. Mechanistically, a series of indirect and direct evidence provide compelling demonstration of MurG as the drug target of murgocil; (a) antisense-based depletion of MurG produces a specific hypersensitization to the compound and reciprocally MurG overexpression confers murgocil resistance, (b) multiple independently derived murgocil resistance mutations isolated in both MRSA and MRSE map to specific residues of MurG, (c) murgocil inhibits MurG-mediated PG lipid II synthesis in a cell-free *in vitro* enzyme assay, and (d) murgocil inhibitory activity is abolished *in vitro* when tested against purified MurG variants containing murgocil resistant amino acid substitution mutations. Further, docking models using the *E. coli* MurG crystal structure and Staphylococcal murgocil resistant MurG mutations suggest murgocil binds to the cleft separating N and C-terminal domains, thereby potentially competing with UDP-GlcNAc substrate binding to this site as well as possibly locking SaMurG into a rigid, nonactive form. Finally, we demonstrate that the synergistic and cidal activity of murgocil in combination with imipenem is achieved, at least in part, by

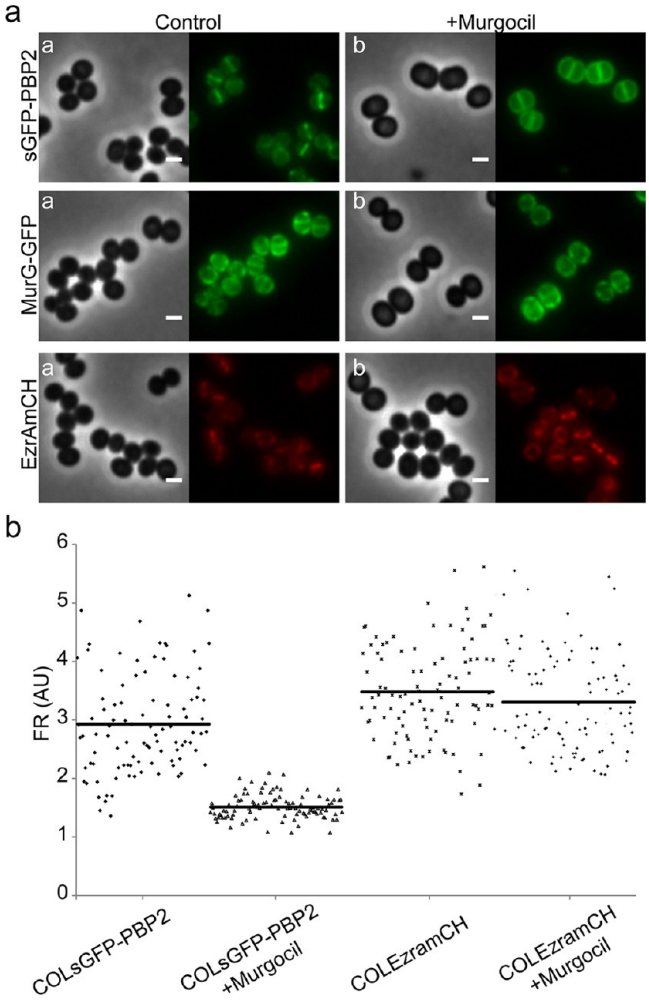

Figure 5. Murgocil affects the recruitment of PBP2 to the division septa. (a) COLsGFP-PBP2 (top panel), COLMurG-GFP (middle panel), and COLEzraAmCh (bottom panel) fluorescence microscopy images of (a) unchallenged control cells and (b) cells challenged with 20 μg/mL of murgocil (5× MIC) for 1 h. Murgocil has an effect on PBP2 recruitment to the division septa when used at concentrations above the MIC (top), whereas control protein EzrA is unaffected by addition of murgocil to growing *S. aureus* cells (bottom). MurG membrane localization appears unaffected by murgocil treatment (middle). Gray panels are phase-contrast images of bacterial cells (white scale bar represents 1 μm), and black panels show the fluorescence images. (b) Quantification of the effect of murgocil on the septal recruitment of sGFP-PBP2 and mCh-EzrA. The fluorescence microscopy images of unchallenged control cells and cells challenged with 20 μg/mL of murgocil (5× MIC) for 1 h were used to quantify the amount of PBP2 and EzrA that is specifically recruited to the division septa. Quantification was performed with 100 cells displaying complete septa for each strain. Horizontal lines correspond to average fluorescence ratio (FR) values. FR values over 2 indicate preferential septal localization while FR values $\leq$2 indicate that a protein is dispersed over the cell surface. FR is calculated by dividing the intensity of fluorescence at the septum by the intensity of fluorescence at the lateral wall (after correction by subtraction of the background).

dx.doi.org/10.1021/cb400487f | *ACS Chem. Biol.* 2013, 8, 2442−2451

mislocalization of PBP2 from the division septum, thus likely reducing β-lactam drug levels necessary to inhibit the residual amount of functionally active PBP2 under murgocil drug treatment conditions.

Despite murgocil targeting a broadly conserved PG biosynthetic enzyme, its microbiological activity is uniquely restricted to Staphylococci, lacking bioactivity against other Gram-positive (e.g., *Bacillus subtilis* and *Streptococcus pyogenes*) or Gram-negative bacteria tested, including *E. coli* and *P. aeruginosa* strains defective in efflux pumps (SI Table 1). Consistent with murgocil bioactivity spectrum, the proposed *S. epidermidis* MurG murgocil binding site is 100% identical to SaMurG, while *B. subtilis* MurG is significantly different, including intrinsic amino acid differences at M45 and D168 (I45 and E168, respectively) (SI Figure 7). Similarly, EcMurG contains a M45L change and *P. aeruginosa* MurG possesses M45L and D168G alterations. These changes alone, being similar (and in the case of D168G, identical) to those found in SaMurG murgocil resistant mutants, are predicted to interfere with murgocil binding and abolish its activity against these orthologous enzymes. Therefore, the narrow spectrum of murgocil appears likely to be MurG-mechanism based. However, further *in vitro* studies using purified MurG from *E. coli* and other recalcitrant bacteria as well as cocrystal structures of murgocil in complex with SaMurG and (ideally) other MurG enzymes are required to fully address this issue. Murgocil also exhibits an unfavorably high rate of spontaneous resistance, in the range $\sim 1 \times 10^{-7}$ at 4× MIC versus standard antibiotics whose frequency of resistance is more typically in the range $\sim 1 \times 10^{-8}$ or lower.[23,27] Therefore, although these issues significantly compromise the antibiotic development potential of murgocil itself, the compound and MurG drug resistance mutations described here now provide important structural modeling-based *in silico* screening opportunities for new MurG inhibitory series with potentially broader activity, reduced susceptibility to resistance, and improved synergistic and cidal activity when paired with β-lactam antibiotics.

Despite historically intensive efforts in identifying target-specific bioactive inhibitors to intracellular steps of PG biosynthesis, it is startling how few molecules have been discovered that meet these basic criteria for an antibiotic drug lead.[23,27,43,44] Generally, these compounds either lack bioactivity and/or solely possess *in vitro* activity against specific Mur enzymes (in which case the inhibitor is either unable to penetrate cells or is efficiently effluxed from cells) and/or their whole cell activity has not been genetically linked to the same enzyme used to screen and identify such inhibitors.[23,27,43] Moreover, in the few exceptions to this generalization, such inhibitors instead act to sequester lipid II PG substrate (e.g., vancomycin, ramoplanin), undecaprenyl-P- (e.g., friulimicin), or undecaprenyl-PP (e.g., bacitracin) rather than directly inhibiting a Mur enzyme.[45−47] Indeed, we are unaware of any report rigorously describing a target-specific bioactive inhibitor to MurG despite attempts using a variety of target or pathway-specific *in vitro* or whole cell screening approaches.[48−52] The potency of murgocil against Staphylococci (MIC 2−4 μg/mL) is, however, considerably lower than the in vitro IC50 (115 μg/mL) of the compound against purified *S. aureus* His-tagged MurG protein. We believe this likely reflects the inability to mimic the *in vivo* complexity of the entire PG synthesizing machinery *in vitro* as well as the difficulty in optimizing an extensive set of conditions tested to effectively solubilize murgocil while still maintaining recombinant MurG *in vitro* enzyme activity. Notwithstanding these technical issues, we provide compelling mechanistic evidence demonstrating that murgocil is both a highly selective and potent inhibitor of endogenous MurG in whole cells. Moreover, murgocil serves as an important addition to the suite of chemical probes[53] to study MurG function, PG synthesis, and its coordinated assembly with other cell wall polymers as well as cytoskeletal and cell division processes in Staphylococci. Importantly, the demonstration that combining phenotypic screens, drug resistant mutant isolation, and mapping by NGS can collectively be used successfully to uncover target-specific bioactive inhibitors of PG biosynthesis provides optimism that additional antibacterial lead series targeting this pathway are expected to be discovered.

METHODS

See Supporting Information for Supplementary Methods for general microbiology, strains and plasmid construction methods.

Accumulation of UDP-*N*-Acetyl-muramoyl-pentapeptide. *S. aureus* SG511 was grown in Mueller-Hinton broth to an OD_{600} of 0.5 and incubated with 130 μg/mL of chloramphenicol for 15 min. Vancomycin (10× MIC, 5 μg/mL) and murgocil (2.5×, 5×, and 10× MIC, 5, 10, 20 μg/mL) were added and incubated for another 30 min. Cells were harvested and extracted with boiling water. The cell extract was centrifuged and the supernatant lyophilized. Nucleotide-linked cell wall precursors were analyzed by HPLC,[54] and corresponding fractions were confirmed by mass spectrometry.

MurG-His$_6$ *In Vitro* Assay Activity. MurG activity was assayed in a final volume of 30 μL containing 2.5 Nmol purified lipid I, 5 nmol UDP-GlcNAc or [^{14}C]UDP-GlcNAc in 60 mM Tris-HCl pH 7.5, 5 mM $MgCl_2$, and 0.5% Triton X-100. Conversion to lipid II was initiated by addition of 0.2 μg of purified MurG-His$_6$ enzyme. The reaction mixture was incubated for 60 min at 30 °C. Lipid intermediates were extracted from the reaction mixture with *n*-butanol/pyridine acetate (2:1, vol/vol), pH 4.2, and analyzed by TLC (silica plates, 60F254; Merck) using chloroform/methanol/water/ammonia (88:48:10:1) as the solvent. Spots were visualized by PMA staining reagent A.[55] Radiolabeled spots were visualized and quantified using a phosphor storage screen and a Storm 820 optical scanner (GE Healthcare, Munich, Germany). Murgocil (molecular mass: 447.582 Da) was added in concentrations ranging from 10 to 500 μM.

Computer Modeling of SaMurG/Murgocil Complex. The compound murgocil 3D conformation was sampled and selected from a set of 3D conformations generated by LigPrep.[56] A steroid bound X-ray structure from PDB was taken to guide the final 3D selection. The X-ray crystal structure of UDP-GlcNAc/EcMurG complex 1NLM.pdb[29] was chosen as the template for the homology model of SaMurG. The alignment from MOE[57] based on sequence similarity was manually adjusted at several regions, in particular, moving a five-residue deletion at F242 out of the uracil binding site. MOE[57] was used to create a homology model that was further refined with Macromodel.[56] Glide[56] and Macromodel[56] were used for docking and complex minimization.

Fluorescence Microscopy. To assess the effect of murgocil at concentrations above the MIC on PBP2, EzrA, and MurG localization, overnight cultures of *S. aureus* strains were diluted 1:500 and grown until $OD_{600\ nm}$ reached 0.3 in tryptic soy broth (TSB, Difco) at 37 °C with aeration. Cultures were then divided into two prewarmed flasks, and murgocil was added at 5× MIC (20 μg/mL) to one of them. Cells were incubated for 1 h at 37 °C with aeration and analyzed by fluorescence microscopy on a thin layer of 1% agarose in phosphate buffered saline. Images were obtained using a Zeiss Axio Observer Z1 microscope equipped with a Photometrics CoolSNAP HQ2 camera (Roper Scientific) using Metamorph software (Meta Imaging series 7.5) and analyzed using ImageJ software.[58] Fluorescence ratios were calculated as previously described.[59]

■ ASSOCIATED CONTENT

Supporting Information

General microbiology, strains and plasmid construction methods, and murgocil chemical synthesis methods. This material is available free of charge via the Internet at http://pubs.acs.org.

■ AUTHOR INFORMATION

Corresponding Author

*Phone: 908-740-2480. E-mail: terry_roemer@merck.com.

Notes

All authors excluding A.M., P.M.P., M.M.S., R.M., K.O., M.G.P., and T.S. are current or past employees of Merck as stated in the affiliations and potentially own stock and/or hold stock options in the company.

■ ACKNOWLEDGMENTS

T.S. and A.M. are supported by the German Research Foundation (DFG, SCHN1284/1-2) and the German Center for Infection Research (DZIF). M.G.P. is funded by ERC-2012-StG-310987 from the European Research Council. P.M.P. was supported by fellowship SFRH/BD/41119/2007 from Fundação para a Ciência e Tecnologia.

■ REFERENCES

(1) van Heijenoort, J. (2001) Recent advances in the formation of the bacterial peptidoglycan monomer unit. *Nat. Prod. Rep. 18*, 503−519.

(2) van Heijenoort, J. (2007) Lipid intermediates in the biosynthesis of bacterial peptidoglycan. *Microbiol. Mol. Biol. Rev. 71*, 620−635.

(3) Scheffers, D. J., and Pinho, M. G. (2005) Bacterial cell wall synthesis: New insights from localization studies. *Microbiol. Mol. Biol. Rev. 69*, 585−607.

(4) Walsh, C. *Antibiotics: Actions, Origins, Resistance* (2003) ASM Press, Washington, DC.

(5) Klevens, R. M., Morrison, M. A., Nadle, J., Petit, S., Gershman, K., Ray, S., Harrison, L. H., Lynfield, R., Dumyati, G., Townes, J. M., Craig, A. S., Zell, E. R., Fosheim, G. E., McDougal, L. K., Carey, R. B., and Fridkin, S. K. (2007) Active bacterial core surveillance (ABCs) MRSA investigators. *JAMA 298*, 1763−1771.

(6) Boucher, H. W., Talbot, G. H., Bradley, J. S., Edwards, J. E., Gilbert, D., Rice, L. B., Scheld, M., Spellberg, B., and Bartlett, J. (2009) Bad bugs, no drugs: No ESKAPE! An update from the Infectious Diseases Society of America. *Clin. Infect. Dis. 48*, 1−12.

(7) Couto, I., de Lencastre, H., Severina, E., Kloos, W., Webster, J. A., Hubner, R. J., Sanches, I. S., and Tomasz, A. (1996) Ubiquitous presence of a *mecA* homologue in natural isolates of *Staphylococcus sciuri*. *Microb. Drug Resist. 2*, 377−391.

(8) de Lencastre, H., Oliveira, D., and Tomasz, A. (2007) Antibiotic resistant *Staphylococcus aureus*: A paradigm of adaptive power. *Curr. Opin. Microbiol. 10*, 428−435.

(9) Fuda, C. C., Fisher, J. F., and Mobashery, S. (2005) β-Lactam resistance in *Staphylococcus aureus*: The adaptive resistance of a plastic genome. *Cell. Mol. Life Sci. 62*, 2617−2633.

(10) Fuda, C., Suvorov, M., Vakulenko, S. B., and Mobashery, S. (2004) The basis for resistance to β-lactam antibiotics by penicillin-binding protein 2a of methicillin-resistant *Staphylococcus aureus*. *J. Biol. Chem. 279*, 40802−40806.

(11) Llarrull, L. I., Fisher, J. F., and Mobashery, S. (2009) Molecular basis and phenotype of methicillin resistance in *Staphylococcus aureus* and insights into new β-lactams that meet the challenge. *Antimicrob. Agents Chemother. 53*, 4051−4063.

(12) Pinho, M. G., de Lencastre, H., and Tomasz, A. (2001) An acquired and a native penicillin binding protein cooperate in building the cell wall of drug-resistant staphylococci. *Proc. Natl. Acad. Sci. U.S.A. 98*, 10886−10891.

(13) Pinho, M. G., Filipe, S. R., de Lencastre, H., and Tomasz, A. (2001) Complementation of the essential peptidoglycan transpeptidase function of penicillin-binding protein 2 (PBP2) by the drug resistance protein PBP2A in *Staphylococcus aureus*. *J. Bacteriol. 183*, 6525−6531.

(14) de Lencastre, H., and Tomasz, A. (1994) Reassessment of the number of auxiliary genes essential for expression of high-level methicillin resistance in *Staphylococcus aureus*. *Antimicrob. Agents Chemother. 38*, 2590−2598.

(15) de Lencastre, H., Wu, S. W., Pinho, M. G., Ludovice, A. M., Filipe, S., Gardete, S., Sobral, R., Gill, S., Chung, M., and Tomasz, A. (1999) Antibiotic resistance as a stress response: Complete sequencing of a large number of chromosomal loci in *Staphylococcus aureus* strain COL that impact on the expression of resistance to methicillin. *Microb. Drug Resist. 5*, 163−175.

(16) Berger-Bächi, B., and Rohrer, S. (2002) Factors influencing methicillin resistance in staphylococci. *Arch. Microbiol. 178*, 165−171.

(17) Lee, S. H., Wang-Jarantow, L., Wang, H., Sillaots, S., Cheng, H., Meredith, T. C., Thompson, J., and Roemer, T. (2011) Antagonism of chemical genetic interaction networks resensitize MRSA to β-lactam antibiotics. *Chem. Biol. 18*, 1379−1389.

(18) Roemer, T., Schneider, T., and Pinho, M. G. (2013) Accessory factors: A chink in the armor of MRSA resistance to β-lactam antibiotics. *Curr. Opin. Microbiol.,*.

(19) Huber, J., Donald, R. G., Lee, S. H., Jarantow, L. W., Salvatore, M. J., Meng, X., Painter, R., Onishi, R. H., Occi, J., Dorso, K., Young, K., Park, Y. W., Skwish, S., Szymonifka, M. J., Waddell, T. S., Miesel, L., Phillips, J. W., and Roemer, T. (2009) Chemical genetic identification of peptidoglycan inhibitors potentiating carbapenem activity against methicillin-resistant *Staphylococcus aureus*. *Chem. Biol. 16*, 837−848.

(20) Tan, C. M., Therien, A. G., Lu, J., Lee, S. H., Caron, A., Gill, C. J., Lebeau-Jacob, C., Benton-Perdomo, L., Monteiro, J. M., Pereira, P. M., Elsen, N. L., Wu, J., Deschamps, K., Petcu, M., Wong, S., Daigneault, E., Kramer, S., Liang, L., Maxwell, E., Claveau, D., Vaillancourt, J., Skorey, K., Tam, J., Wang, H., Meredith, T. C., Sillaots, S., Wang-Jarantow, L., Ramtohul, Y., Langlois, E., Landry, F., Reid, J. C., Parthasarathy, G., Sharma, S., Baryshnikova, A., Lumb, K. J., Pinho, M. G., Soisson, S. M., and Roemer, T. (2012) Restoring methicillin-resistant *Staphylococcus aureus* susceptibility to β-lactam antibiotics. *Sci. Transl. Med. 4*, 126ra35.

(21) Koyama, N., Tokura, Y., Münch, D., Sahl, H. G., Schneider, T., Shibagaki, Y., Ikeda, H., and Tomoda, H. (2012) The nonantibiotic small molecule cyslabdan enhances the potency of β-lactams against MRSA by inhibiting pentaglycine interpeptide bridge synthesis. *PLoS One 7*, e48981.

(22) Therien, A. G., Huber, J. L., Wilson, K. E., Beaulieu, P., Caron, A., Claveau, D., Deschamps, K., Donald, R. G., Galgoci, A. M., Gallant, M., Gu, X., Kevin, N. J., Lafleur, J., Leavitt, P. S., Lebeau-Jacob, C., Lee, S. S., Lin, M. M., Michels, A. A., Ogawa, A. M., Painter, R. E., Parish, C. A., Park, Y. W., Benton-Perdomo, L., Petcu, M., Phillips, J. W., Powles, M. A., Skorey, K. I., Tam, J., Tan, C. M., Young, K., Wong, S., Waddell, S. T., and Miesel, L. (2012) Broadening the spectrum of β-lactam antibiotics through inhibition of signal peptidase type I. *Antimicrob. Agents Chemother. 56*, 4662−4670.

(23) Silver, L. L. (2013) Viable screening targets related to the bacterial cell wall. *Ann. N.Y. Acad. Sci. 277*, 29−53.

(24) Isono, K., Uramoto, M., Kusakabe, H., Kimura, K., Isaki, K., Nelson, C. C., and McCloskey, J. A. (1985) Liposidomycins: Novel nucleoside antibiotics which inhibit bacterial peptidoglycan synthesis. *J. Antibiot. 38*, 1617−1621.

(25) Kimura, K.-I., Miyata, N., Kawanishi, G., Kamio, Y., Izaki, K., Isono, and K. (1989) Liposidomycin C inhibits phospho-N-acetylmuramyl-pentapeptide transferase in peptidoglycan synthesis of *Escherichia coli* Y-10. *Agric. Biol. Chem. 53*, 1811−1815.

(26) Brandish, P. E., Burnham, M. K., Lonsdale, J. T., Southgate, R., Inukai, M., and Bugg, T. D. (1996) Slow-binding inhibition of phospho-N-acetylmuramyl-pentapeptide translocase (*Escherichia coli*) by mureidomycin A. *J. Biol. Chem. 271*, 7609−7614.

(27) Silver, L. L. (2011) Challenges of antibacterial discovery. *Clin. Microbiol. Rev. 24*, 71−109.
(28) Ha, S., Walker, D., Shi, Y., and Walker, S. (2000) The 1.9 A crystal structure of *Escherichia coli* MurG, a membrane-associated glycosyltransferase involved in peptidoglycan biosynthesis. *Protein Sci. 9*, 1045−1052.
(29) Hu, Y., Chen, L., Ha, S., Gross, B., Falcone, B., Walker, D., Mokhtarzadeh, M., and Walker, S. (2003) Crystal structure of the MurG:UDP-GlcNAc complex reveals common structural principles of a superfamily of glycosyltransferases. *Proc. Natl. Acad. Sci. U.S.A. 100*, 845−849.
(30) Campbell, J., Singh, A. K., Santa Maria, J. P., Kim, Y., Brown, S., Swoboda, J. G., Mylonakis, E., Wilkinson, B., and Walker, S. (2011) Synthetic lethal compound combinations reveal a fundamental connection between wall teichoic acid and peptidoglycan biosyntheses in *Staphylococcus aureus*. *ACS Chem. Biol. 6*, 106−116.
(31) Brown, S., Xia, G., Luhachack, L. G., Campbell, J., Meredith, T. C., Chen, C., Winstel, V., Gekeler, C., Irazoqui, J. E., Peschel, A., and Walker, S. (2012) Methicillin resistance in *Staphylococcus aureus* requires glycosylated wall teichoic acids. *Proc. Natl. Acad. Sci. U.S.A. 109*, 18909−18914.
(32) Weidenmaier, C., and Peschel, A. (2008) Teichoic acids and related cell-wall glycopolymers in Gram-positive physiology and host interactions. *Nat. Rev. Microbiol. 6*, 276−287.
(33) Swoboda, J. G., Campbell, J., Meredith, T. C., and Walker, S. (2010) Wall teichoic acid function, biosynthesis, and inhibition. *ChemBioChem 11*, 35−45.
(34) Meredith, T. C., Wang, H., Beaulieu, P., Gründling, A., and Roemer, T. (2012) Harnessing the power of transposon mutagenesis for antibacterial target identification and evaluation. *Mobil Genet. Elem. 2*, 171−178.
(35) Farha, M. A., Leung, A., Sewell, E. W., D'Elia, M. A., Allison, S. E., Ejim, L., Pereira, P. M., Pinho, M. G., Wright, G. D., and Brown, E. D. (2013) Inhibition of WTA synthesis blocks the cooperative action of PBPs and sensitizes MRSA to β-lactams. *ACS Chem. Biol. 8*, 226−233.
(36) Donald, R. G., Skwish, S., Forsyth, R. A., Anderson, J. W., Zhong, T., Burns, C., Lee, S., Meng, X., LoCastro, L., Jarantow, L. W., Martin, J., Lee, S. H., Taylor, I., Robbins, D., Malone, C., Wang, L., Zamudio, C. S., Youngman, P. J., and Phillips, J. W. (2009) A *Staphylococcus aureus* fitness test platform for mechanism-based profiling of antibacterial compounds. *Chem. Biol. 16*, 826−836.
(37) Wang, H., Gill, C. J., Lee, S. H., Mann, P., Zuck, P., Meredith, T. C., Murgolo, N., She, X., Kales, S., Liang, L., Liu, J., Wu, J., Santa Maria, J., Su, J., Pan, J., Hailey, J., Mcguinness, D., Tan, C. M., Flattery, A., Walker, S., Black, T., and Roemer, T. (2013) Discovery of novel wall teichoic acid inhibitors as effective anti-MRSA β-lactam combination agents. *Chem. Biol. 20*, 272−284.
(38) Schneider, T., Kruse, T., Wimmer, R., Wiedemann, I., Sass, V., Pag, U., Jansen, A., Nielsen, A. K., Mygind, P. H., Raventós, D. S., Neve, S., Ravn, B., Bonvin, A. M., De Maria, L., Andersen, A. S., Gammelgaard, L. K., Sahl, H. G., and Kristensen, H. H. (2010) Plectasin, a fungal defensin, targets the bacterial cell wall precursor Lipid II. *Science 328*, 1168−1172.
(39) Pinho, M. G., and Errington, J. (2005) Recruitment of penicillin-binding protein PBP2 to the division site of *Staphylococcus aureus* is dependent on its transpeptidation substrates. *Mol. Microbiol. 55*, 799−807.
(40) Adams, D. W., and Errington, J. (2009) Bacterial cell division: Assembly, maintenance, and disassembly of the Z ring. *Nat. Rev. Microbiol. 7*, 642−653.
(41) Pinho, M. G., and Errington, J. (2003) Dispersed mode of *Staphylococcus aureus* cell wall synthesis in the absence of the division machinery. *Mol. Microbiol. 50*, 871−881.
(42) Jorge, A. M., Hoiczyk, E., Gomes, J. P., and Pinho, M. G. (2011) EzrA contributes to the regulation of cell size in *Staphylococcus aureus*. *PLoS One 6*, e27542.
(43) Silver, L. L. (2003) Novel inhibitors of bacterial cell wall synthesis. *Curr. Opin. Microbiol. 6*, 431−438.
(44) Payne, D. J., Gwynn, M. N., Holmes, D. J., and Pompliano, D. L. (2007) Drugs for bad bugs: Confronting the challenges of antibacterial discovery. *Nat. Rev. Drug Discov. 6*, 29−40.
(45) Hu, Y., Helm, J. S., Chen, L., Ye, X. Y., and Walker, S. (2003) Ramoplanin inhibits bacterial transglycosylases by binding as a dimer to lipid II. *J. Am. Chem. Soc. 125*, 8736−8737.
(46) Silver, L. L. (2006) Does the cell wall of bacteria remain a viable source of targets for novel antibiotics? *Biochem. Pharmacol. 71*, 996−1005.
(47) Schneider, T., Gries, K., Josten, M., Wiedemann, I., Pelzer, S., Labischinski, H., and Sahl, H. G. (2009) The lipopeptide antibiotic Friulimicin B inhibits cell wall biosynthesis through complex formation with bactoprenol phosphate. *Antimicrob. Agents Chemother. 53*, 1610−1618.
(48) Helm, J. S., Hu, Y., Chen, L., Gross, B., and Walker, S. (2003) Identification of active-site inhibitors of MurG using a generalizable, high-throughput glycosyltransferase screen. *J. Am. Chem. Soc. 125*, 11168−11169.
(49) Hu, Y., Helm, J. S., Chen, L., Ginsberg, C., Gross, B., Kraybill, B., Tiyanont, K., Fang, X., Wu, T., and Walker, S. (2004) Identification of selective inhibitors for the glycosyltransferase MurG via high-throughput screening. *Chem. Biol. 11*, 703−711.
(50) Barbosa, M. D., Ross, H. O., Hillman, M. C., Meade, R. P., Kurilla, M. G., and Pompliano, D. L. (2002) A multitarget assay for inhibitors of membrane-associated steps of peptidoglycan biosynthesis. *Anal. Biochem. 306*, 17−22.
(51) Barbosa, M. D., Yang, G., Fang, J., Kurilla, M. G., and Pompliano, D. L. (2002) Development of a whole-cell assay for peptidoglycan biosynthesis inhibitors. *Antimicrob. Agents Chemother. 46*, 943−946.
(52) DeCenzo, M., Kuranda, M., Cohen, S., Babiak, J., Jiang, Z. D., Su, D., Hickey, M., Sancheti, P., Bradford, P. A., Youngman, P., Projan, S., and Rothstein, D. M. (2002) Identification of compounds that inhibit late steps of peptidoglycan synthesis in bacteria. *J. Antibiot. 55*, 288−295.
(53) Foss, M. H., Eun, Y. J., and Weibel, D. B. (2011) Chemical-biological studies of subcellular organization in bacteria. *Biochemistry 50*, 7719−7734.
(54) Rubinchik, E., Schneider, T., Elliott, M., Scott, W. R., Pan, J., Anklin, C., Yang, H., Dugourd, D., Müller, A., Gries, K., Straus, S. K., Sahl, H. G., and Hancock, R. E. (2011) Mechanism of Action and limited cross-resistance of new lipopeptide MX-2401. *Antimicrob. Agents Chemother. 55*, 2743−2754.
(55) Schneider, T., Senn, M. M., Berger-Bächi, B., Tossi, A., Sahl, H. G., and Wiedemann, I. (2004) *In vitro* assembly of a complete, pentaglycine interpeptide bridge containing cell wall precursor (lipid II-Gly5) of *Staphylococcus aureus*. *Mol. Microbiol. 53*, 675−685.
(56) *LigPrep* Glide, Macromodel (2012) Schrödinger, LLC, New York.
(57) *MOE, Molecular Operating Environment*, 2012.10 (2012) Chemical Computing Group Inc., Montreal, QC, Canada.
(58) Abràmoff, M. D., Magalhães, P. J., and Ram, S. J. (2004) Image processing with ImageJ. *Biophotonics Int. 11*, 36−42.
(59) Pereira, P. M., Filipe, S. R., Tomasz, A., and Pinho, M. G. (2007) Fluorescence ratio imaging microscopy shows decreased access of vancomycin to cell wall synthetic sites in vancomycin-resistant *Staphylococcus aureus*. *Antimicrob. Agents Chemother. 51*, 3627−3633.